

General Disclaimer

One or more of the Following Statements may affect this Document

- This document has been reproduced from the best copy furnished by the organizational source. It is being released in the interest of making available as much information as possible.
- This document may contain data, which exceeds the sheet parameters. It was furnished in this condition by the organizational source and is the best copy available.
- This document may contain tone-on-tone or color graphs, charts and/or pictures, which have been reproduced in black and white.
- This document is paginated as submitted by the original source.
- Portions of this document are not fully legible due to the historical nature of some of the material. However, it is the best reproduction available from the original submission.

NASA
Technical
Memorandum

NASA TM-82538



IMAGE MOTION COMPENSATION BY AREA CORRELATION AND
CENTROID TRACKING OF SOLAR SURFACE FEATURES

By M. E. Nein, W. R. McIntosh, and N. P. Cumings

July 1983

(NASA-TM-82538) IMAGE MOTION COMPENSATION
BY AREA CORRELATION AND CENTROID TRACKING OF
SOLAR SURFACE FEATURES (NASA) 17 p
HC A02/MF A01

N83-32690

CSCC USA

Unclas
G3/89 28486



National Aeronautics and
Space Administration

George C. Marshall Space Flight Center

1. REPORT NO. NASA TM 82538	2. GOVERNMENT ACCESSION NO.	3. RECIPIENT'S CATALOG NO.	
4. TITLE AND SUBTITLE Image Motion Compensation by Area Correlation and Centroid Tracking of Solar Surface Features		5. REPORT DATE July 1983	6. PERFORMING ORGANIZATION CODE
		8. PERFORMING ORGANIZATION REPORT #	
7. AUTHOR(S) M. E. Nim, W. R. McIntosh, and N. P. Cummings		10. WORK UNIT NO.	
9. PERFORMING ORGANIZATION NAME AND ADDRESS George C. Marshall Space Flight Center Marshall Space Flight Center, Alabama 35812		11. CONTRACT OR GRANT NO.	
		13. TYPE OF REPORT & PERIOD COVERED Technical Memorandum	
12. SPONSORING AGENCY NAME AND ADDRESS National Aeronautics and Space Administration Washington, D.C. 20546		14. SPONSORING AGENCY CODE	
		15. SUPPLEMENTARY NOTES Prepared by Advanced Systems Office.	
16. ABSTRACT An experimental solar correlation tracker has been tested and evaluated on a ground-based solar magnetograph. Using sunspots as fixed targets, tracking error signals were derived by which the telescope image was stabilized against wind induced perturbations. Two methods of stabilization were investigated; mechanical stabilization of the image by controlled two-axis motion of an active optical element in the telescope beam, and electronic stabilization by biasing of the electron scan in the recording camera. Both approaches have demonstrated telescope stability of about 0.6 arc sec under random perturbations which can cause the unstabilized image to move up to 120 arc sec at frequencies up to 30 Hz.			
17. KEY WORDS Image motion compensation Solar telescope stabilization Aim point target tracking Sunspots/solar granules tracking		18. DISTRIBUTION STATEMENT Unclassified Unlimited	
19. SECURITY CLASSIF. (of this report) Unclassified	20. SECURITY CLASSIF. (of this page) Unclassified	21. NO. OF PAGES 17	22. PRICE NTIS

ACKNOWLEDGMENTS

This project was sponsored by the MSFC Center Director's Discretionary Fund Program. The authors gratefully acknowledge the assistance and encouragement provided by the Discretionary Program review committee.

TABLE OF CONTENTS

	Page
INTRODUCTION.....	1
SYSTEM DESCRIPTION.....	2
Tracker.....	3
Active Optical Image Stabilizer.....	5
SOLAR MAGNETOGRAPH AND TRACKER INTEGRATION.....	5
CORRELATION TRACKER TESTING AND EVALUATION.....	6
ALTERNATE SYSTEM.....	8
CONCLUSION.....	11
REFERENCES.....	12

~~PRECEDING PAGE BLANK NOT FILMED~~

LIST OF ILLUSTRATIONS

Figure	Title	Page
1a.	Solar vector magnetograph and correlation tracker schematic.....	2
1b.	Tracker assembly and optical image stabilization element.....	2
2.	Correlation tracker system block diagram.....	3
3.	Sunspots and tracker scan patterns.....	3
4.	Schematic sunspot image on photocathode and analog video output.....	4
5.	Image displacement versus tilt angle for a 1-in. thick BK-7 glass plate.....	5
6.	Typical magnetograms without (a) and with (b) correlation tracker stabilization.....	6
7.	Magnetic field contours acquired with correlation tracker assistance.....	7
8.	Correlation tracker usage in support of Solar Maximum Mission flight.....	8
9.	Electronic stabilization block diagram.....	9
10.	Sunspot images with (a) and without (b) electronic stabilization.....	9
11.	Micro-densitometer scans of sunspot film images.....	10
12.	Enlargement of section A-A in Figure 11 showing image instability.....	10

TECHNICAL MEMORANDUM

IMAGE MOTION COMPENSATION BY AREA CORRELATION AND CENTROID TRACKING OF SOLAR SURFACE FEATURES

INTRODUCTION

Intensive solar astronomy research has rapidly advanced the knowledge and understanding of the physical processes that take place in the Sun. As this research continues, the emphasis naturally focuses on obtaining higher instrument resolution, requiring larger apertures.

Now that the Space Shuttle is operational, it will be possible to place into orbit solar telescopes with primary apertures of 1 to 2 m in diameter. These advanced high resolution instruments will in turn require that the images be stabilized to sub-arcsecond accuracies. The techniques currently used for stabilization of space solar instruments generally depend on sensing the angular orientation of the rapid change in brightness of the Sun's disc at the limb for use as angular reference. This technique which was used in the Apollo Telescope Mount (ATM) Fine Sun Sensor is adequate for telescope stability tolerances of near 1.0 arcsec, but is limited to tracking accuracies of approximately 2.0 arcsec by the constant activity within the solar atmosphere, shifting the location of the limb as the solar energy moves radially outward.

To overcome the limitations of solar limb tracking for pointing and stabilization, other concepts have been investigated which use more clearly defined, stable solar surface features to derive error signals for the stabilization system. In the early 1970's the technology for "aim-point" target recognition had been developed for defense systems. This method of target or correlation tracking appeared to be applicable to solar telescope stabilization using solar surface features such as granules and sunspots as targets for the error signal generation. Since this technique derives the control signals from the same telescope image that is used for scientific data acquisition, any problem of relative displacement or misalignment of the tracker components is avoided. Misalignment normally occurs because of structural deformations due to thermal and mechanical perturbations if two independent optical systems are used.

The potential advantages of aim point target recognition for stabilization of spaceborne solar telescopes led MSFC to initiate a breadboard development effort in 1972 to build and test such a tracking system in the laboratory. Recent resumption of this development effort, using a groundbased telescope for simulation of random image motion, resulted in the final verification of the concept feasibility. This development phase produced an experimental solar correlation tracking system which is now routinely used to stabilize solar images of a ground-based telescope to ± 0.6 arcsec against wind-induced perturbations of the telescope's line-of-sight. The measured stability actually exceeds the resolution of the magnetograph which is limited by the vidicon camera resolution to about 2.5 arcsec. The random image motion caused by wind loading and atmospheric perturbations in these tests simulate random image motion which could be caused in a typical space-based telescope by thermal and structural deformations, camera drives, astronaut activities and spacecraft maneuvers.

SYSTEM DESCRIPTION

ORIGINAL PAGE IS
OF POOR QUALITY

The tracking system, mounted on a solar telescope, is schematically shown in Figure 1a. The two major elements are the tracker assembly and the active optical image stabilizer as shown in Figure 1b.

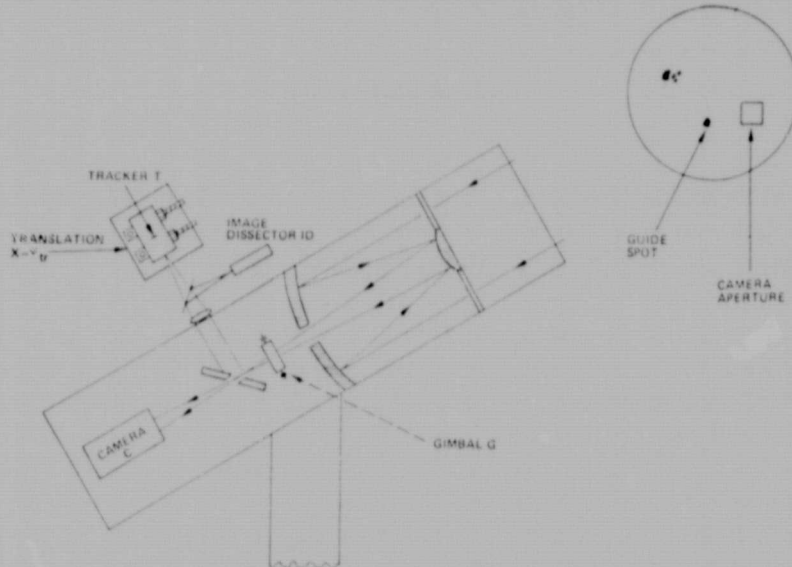
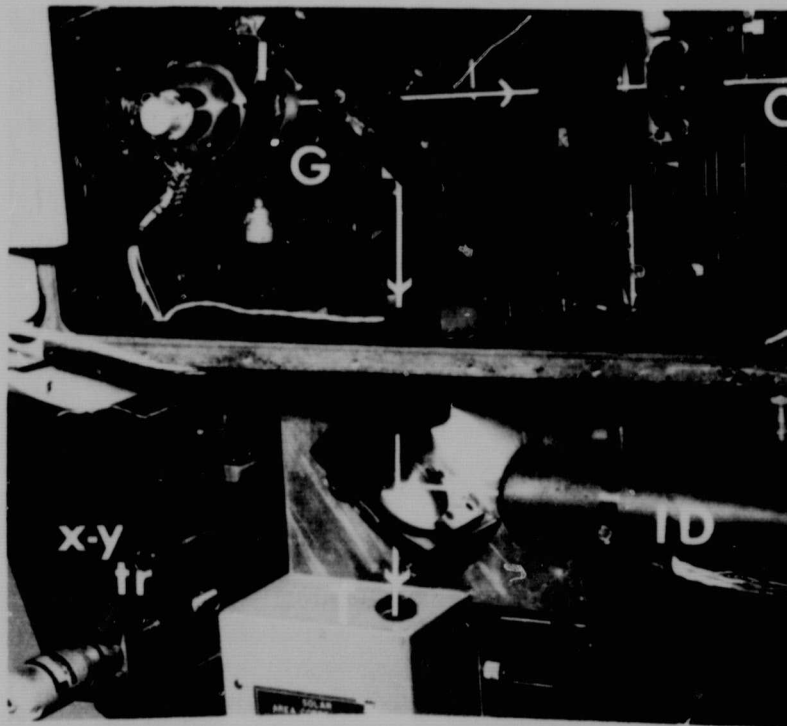


Figure 1a. Solar vector magnetograph and correlation tracker schematic.



G = Gimbal; I = Image Stabilizer; C = To Camera; T = Tracker Assembly; ID = Image Dissector; $x-y_{tr}$ = Translation Stage.

Figure 1b. Tracker assembly and optical image stabilization element.

Tracker

The two tracking modes which are possible with the tracking system are a correlation mode and a radiometric balance mode. In the correlation mode, the tracker functions by scanning a scene, storing the video image, and then comparing a real-time scan with the stored image to generate an X-Y error signal.

A portion of the solar image is incident on the photocathode of an image dissector (F4012) sensor where photons are converted to electrons. The electron image is amplified and first sent to an analog-to-digital converter and then to a storage register (Fig. 2). Once the storage register is loaded, the signal is gated to the correlation computer. By use of an algorithm, an error signal is obtained. This signal passes through a Digital-to-Analog Converter to the deflection drivers, which position the electron image to keep it centered on the stored image. The tracker uses a circular scan to generate the scene information. In the store mode, the scan is stepped first to the center, followed by up, down, left and right motion with one complete circular scan for each position. Figure 3 shows a typical solar image with granule and sunspot surface features and tracker scan patterns. Each scan divides the scene into 66 elements. Thus, the stored information contains a total of 330 elements. Figure 4 is a schematic representation of a sunspot image on the photocathode. The scan rate is 1.0 kHz.

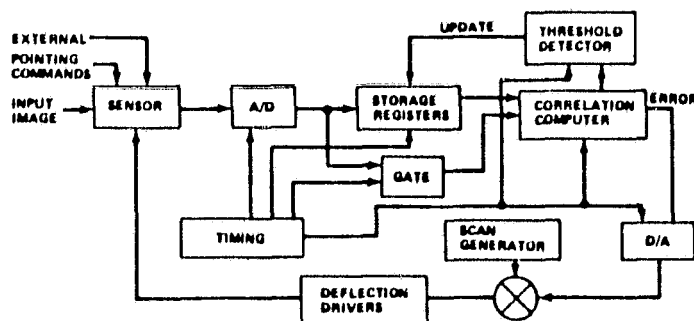


Figure 2. Correlation tracker system block diagram.

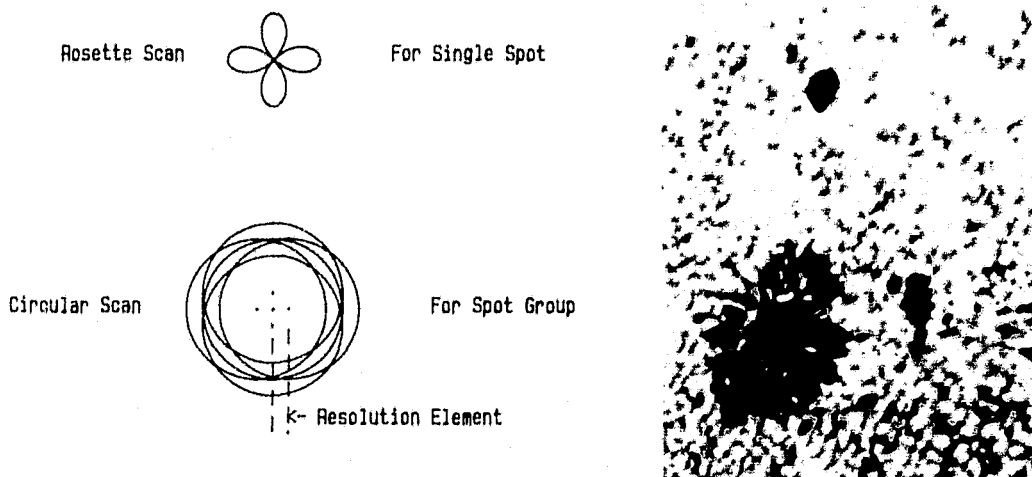


Figure 3. Sunspots and tracker scan patterns.

ORIGINAL PAGE IS
OF POOR QUALITY

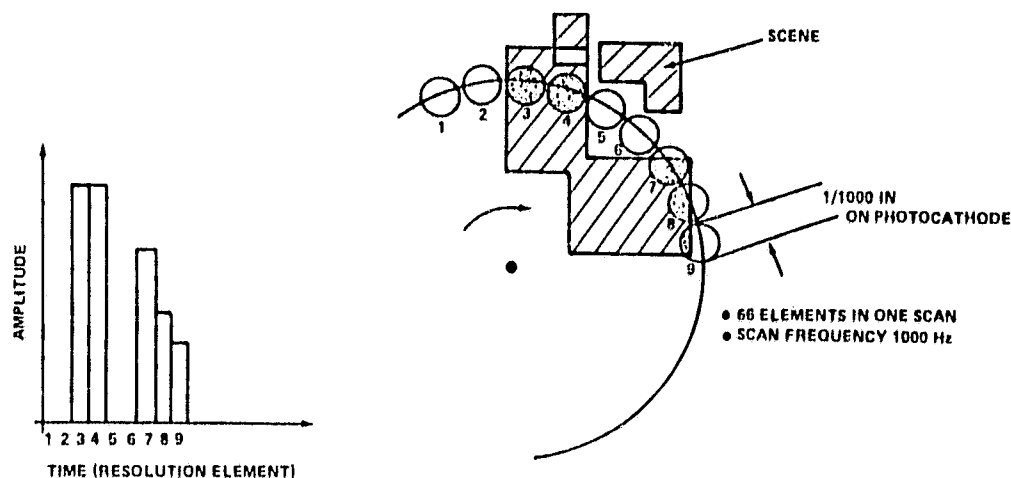


Figure 4. Schematic sunspot image on photocathode and analog video output.

The error is obtained from a product look-up table and is derived from the following approximations:

$$\text{Elevation Error} = \int (Y_i X_{Bi} - Y_i X_{Ci}) dt ,$$

where Y_i , X_{Bi} and X_{Ci} are target scene scan data, reference up-scan data, and reference down-scan data, respectively.

$$\text{Azimuth Error} = \int (Y_i X_{Di} - Y_i X_{Ei}) dt ,$$

where X_{Di} and X_{Ei} represent right and left scan data, respectively.

This computation derives the necessary error curve and sensing for closed-loop tracking. These errors are then applied to the sensor deflection coils for closed-loop sensor tracking.

The correlation tracker in the circular scan mode requires multispot groups for tracking as previously shown in Figure 3. However, at times the activity on the Sun is very low, and only single sunspots can be observed. Therefore, a different tracking mode is needed for those conditions.

A simplified rosette scan was added so that the tracker could dissect the image of a single spot (shown also in Fig. 3) to generate an error signal. This mode operates by deflecting the tube's aperture a small amount in the horizontal and vertical directions such that the spot scans in and out of the tube's aperture. By forcing the output of the positive horizontal image equal to the negative horizontal image and the positive vertical image equal to the negative vertical image, the aperture of the tube is centered on the sunspot's image. Inverting the video signal of the sunspot and surrounding area, a tracking scheme of radiant energy balance tracking (radiometric balance) is obtained whereby a single spot generates an error signal which may be used for telescope guiding.

The error signal generated for closed-loop sensor tracking is forced to zero through the use of an active optical image stabilizer which displaces the image such that zero tracker error is maintained. The active optical element as shown in Figure 1b consists of a two-axis gimbal system with a 1-in. thick flat optical refractive element. This element, which is positioned in the optical beam of the telescope, is used to translate the image in the focal plane by use of the refractive properties of the glass (Fig. 5) in conjunction with a controlled tilt of the element. The amount of tilt is commanded by the tracker error signal and gimbal electronics so that the line-of-sight at the camera is forced to zero.

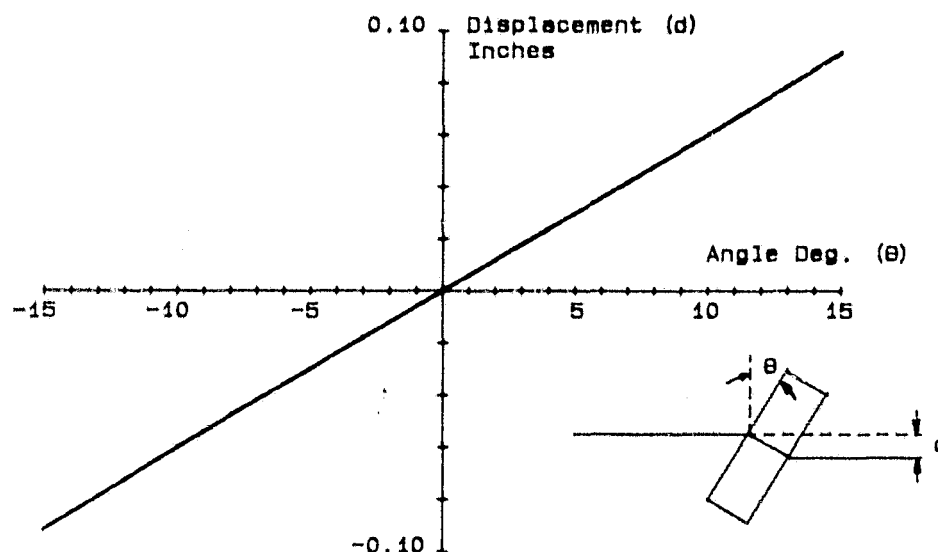


Figure 5. Image displacement versus tilt angle for a 1-in. thick BK-7 glass plate.

SOLAR MAGNETOGRAPH AND TRACKER INTEGRATION

The MSFC Solar Vector Magnetograph is used to make observations of the Sun's vector magnetic fields. The data is obtained by consecutively digitizing video images of both circular and linearly polarized light. Magnetic field strengths are derived from the data using various standard solar modeling techniques. The magnetograph uses an $f/13$ Cassegrain telescope of 30 cm aperture to present a 5×5 arcmin image of the Sun ($\cong 1/6$ total diameter) to a sec vidicon camera. Resolution of the camera is 2.5 arcsec. The tracker is coupled to the telescope's optical beam via an optical fold mirror and lens system (Fig. 1). The tracker is mounted on an X-Y translation stage which allows offset pointing by aligning the science camera field-of-view and the tracker field-of-view such that offset guiding is accomplished.

Before the engagement of the solar correlation tracking loop, the telescope is pointed to the radiometric center of the Sun with a limb guider. Under ideal unperturbed conditions, this guider will point the system with an accuracy of 2 arcmin, with a stability of 9.0 arcsec.

CORRELATION TRACKER TESTING AND EVALUATION

Testing and evaluation of the solar correlation tracker were conducted at the magnetograph telescope. Wind-induced random perturbations of the telescope's line-of-sight were used to evaluate the response of the correlation tracker stabilization.

On a typical day, wind and atmospheric perturbations cause the magnetograph image to move by as much as 120 arcsec in a single axis with a frequency of 30 Hz if the telescope is stabilized with a limb guider. Frequently, the perturbations can even reach such levels that solar observations are not possible at all without image motion stabilization. Considerable improvement of the image stability is, however, obtained when the correlation tracker is engaged in the loop. Figure 6 shows typical data obtained on two different days without (a), and with (b) image stabilization by the correlation tracker. The photographs of the digital image clearly show the increase in resolution obtained on a windy day with the correlation tracker. These photographs were created by alternately adding 256 left and right circularly polarized digital images and subtracting the integrated images from each other.

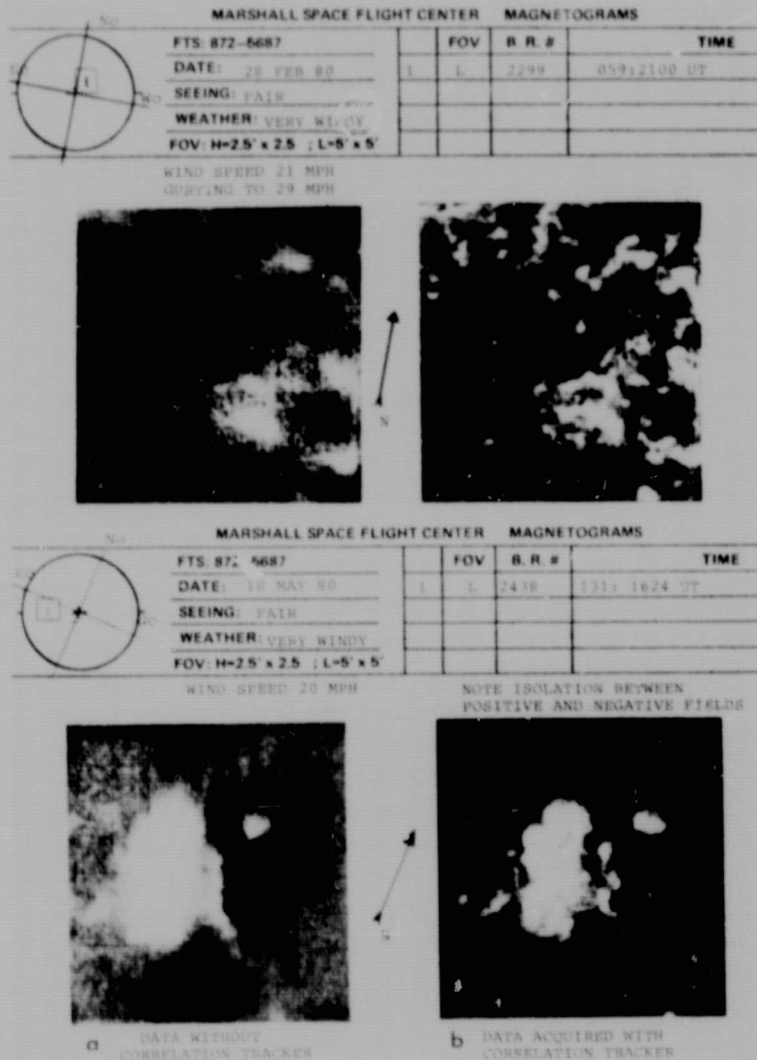


Figure 6. Typical magnetograms without (a) and with (b) correlation tracker stabilization.

ORIGINAL PAGE IS
OF POOR QUALITY

The integration time for each image is 33 msec and the time required to obtain the data for the processed frame is approximately 30 sec. It is clearly evident that motion of the telescope caused by the wind during the multiple exposures (a) degraded the data to the point where they are considered unusable. Conversely, use of the correlation tracker to stabilize the image allowed quite usable data to be acquired under these very adverse conditions (b). Image smearing was reduced from an estimated 20 arcsec or greater to less than the magnetograph pixel resolution of 2.5 arcsec.

Figure 7 is a computer-generated contour plot of longitudinal magnetograph data, acquired with the assistance of the correlation tracker, showing strong gradients between the positive and negative magnetic fields (solid lines and dashes). The strength of these gradients is very important in predicting solar flare activity. When the images were not stabilized using the correlation tracker, smearing of the data caused the gradients to appear so weak that the data was not useful and thus not recorded.

MARSHALL SPACE FLIGHT CENTER MAGNETOGRAMS
TELEPHONE: 205-453-5687 FTS: 872-5687

FILTERED LONGITUDINAL PLOT
TIME 131113:46:25
ZEISS FILTER: 872 ENHANCEMENTS: 255
EXPOSURE: 1.15 POLARIZATIONS: 1
XPOS: -5.13 YPOS: -0.60
APERTURE: X(20,110) Y(20,110)

LABEL	VALUE	LABEL	VALUE
A	1	M	-1
B	10	I	-10
C	25	J	-25
D	50	K	-50
E	100	L	-100
F	150	H	-150
G	200	N	-200

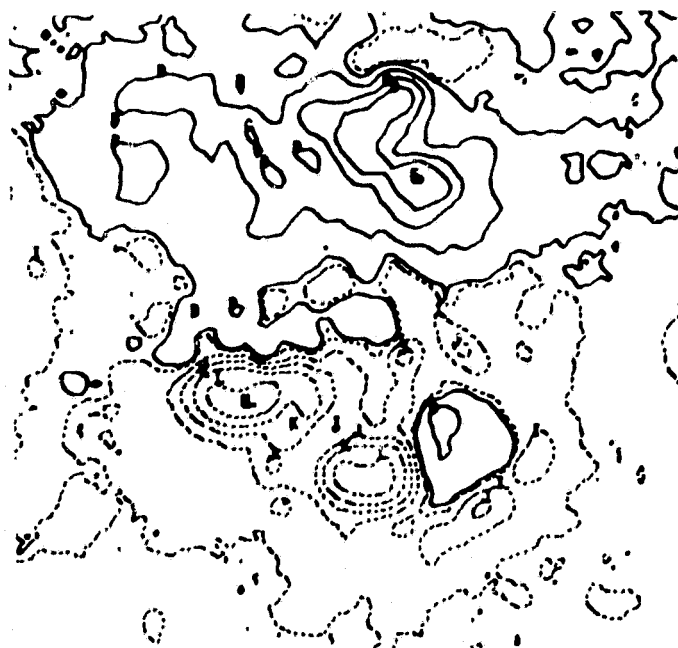


Figure 7. Magnetic field contours acquired with correlation tracker assistance.

As a result of the installation of the solar area correlation tracker on the magnetograph in late 1979, high resolution magnetograms can be obtained routinely even on very windy days. Figure 8 shows the use of the correlation trackers during a typical observation period: during 33 days (April-May 1980) when observations were made, wind perturbation would have absolutely prohibited operation for 12 days without the stabilization afforded by the tracker. The correlation tracker thus increased observation time by 36 percent.

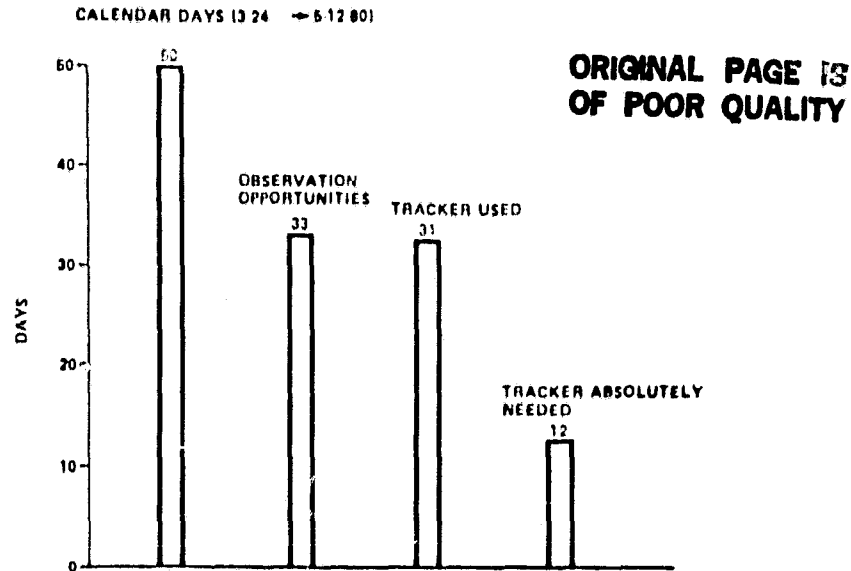


Figure 8. Correlation tracker usage in support of Solar Maximum Mission flight.

ALTERNATE SYSTEM

During development and testing of the correlation tracker, it became apparent that the system is frequency-limited by the mechanical response of the gimbal motors driving the active optical image stabilizer. Typically, the gimbal and closed-loop response has a bandwidth of 18 Hz on the inner gimbal and 23 Hz on the outer gimbal. Although this response is more than adequate for most space applications, it would be desirable to avoid the use of mechanical gimbals and actuators. Thus, a method of electronic stabilization was conceived and developed.

This approach is based on a quasi-closed loop technique which does not utilize any mechanical motion. The solar tracker is locked on a sunspot which it tracks anywhere in its image area. The X-Y error signals are then applied to the deflection system of a co-located camera such that a raster scan area remains stationary on the viewing screen. This is accomplished by subtracting any image motion from the image sensed by the co-located camera.

The block diagram for this system is depicted in Figure 9. This method has demonstrated an image stability ranging from ± 0.3 to ± 0.7 arcsec as compared with ± 0.6 arcsec stability obtained with the mechanical tracker. However, the frequency response of the system is increased to about 50 Hz, which is the response of the particular tracker electronics. With a new design of the tracker, the bandwidth could be further increased to at least 100 Hz. Data taken with this system are shown in Figure 10, which depicts CRT displays of a sunspot group with and without stabilization of the image. Both pictures were taken with a 2 sec exposure with an induced motion of ± 47 arcsec in the horizontal axis.

ORIGINAL PAGE IS
OF POOR QUALITY

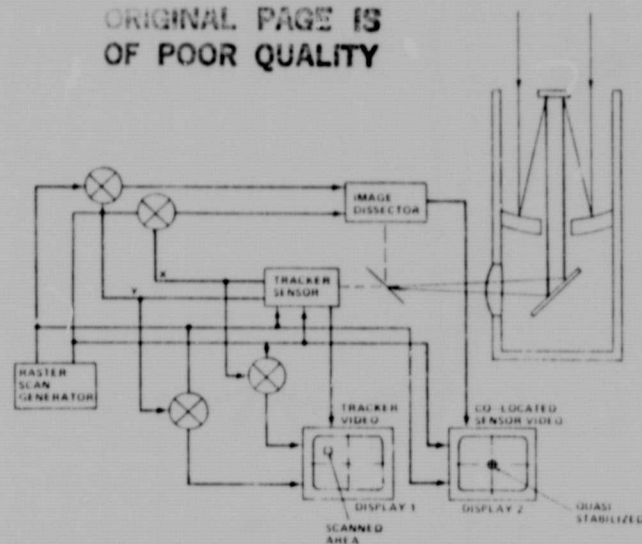


Figure 9. Electronic stabilization block diagram.

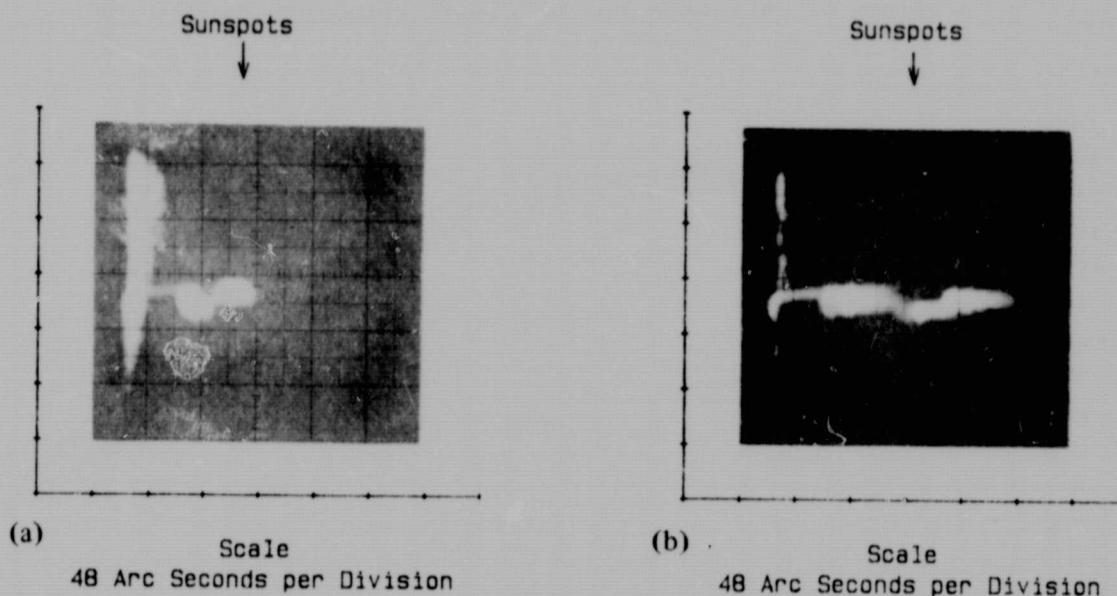


Figure 10. Sunspot images with (a) and without (b) electronic stabilization.

The bright areas near the center are the sunspots. Figure 10a shows the sunspot group with the tracker loop closed. Figure 10b shows the resultant smear caused by the induced motion without closed-loop control. Similar data was recorded on 16 mm movie film for analysis using a micro-densitometer.

Figure 11 shows the film density profile of the two sunspots as a function of the angular size and frame-to-frame displacement caused by the residual motion in the closed loop tracker configuration. This information was enlarged in Section AA, Figure 12, to determine the maximum frame-to-frame image displacement. The maximum stability error remaining in the image is ± 0.7 arcsec.

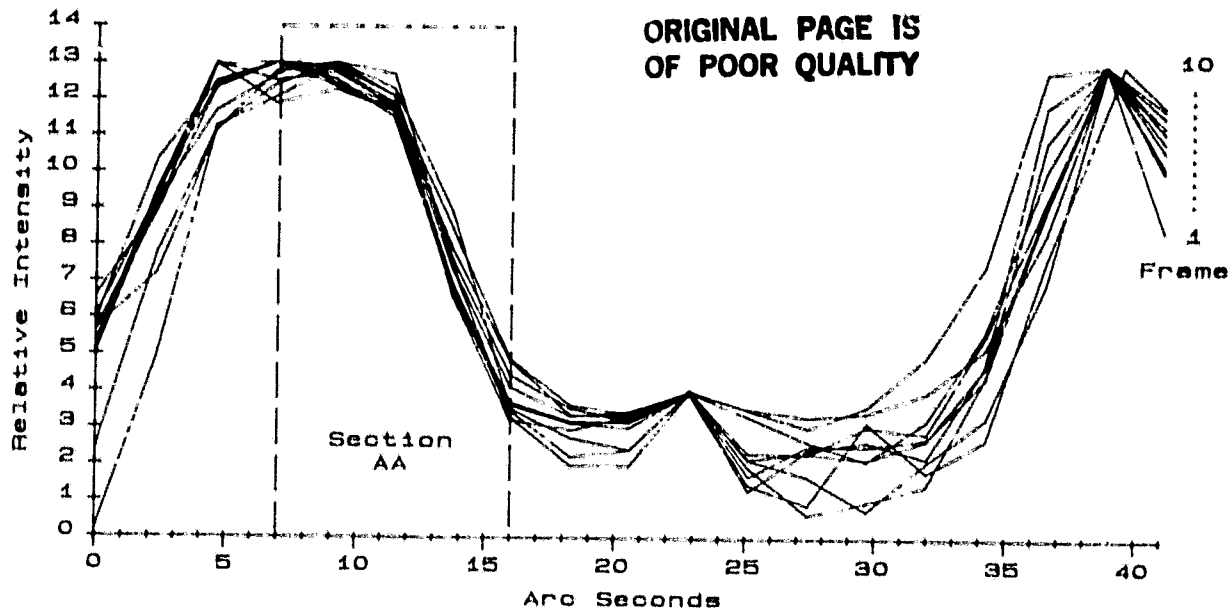


Figure 11. Micro-densitometer scans of sunspot film images.

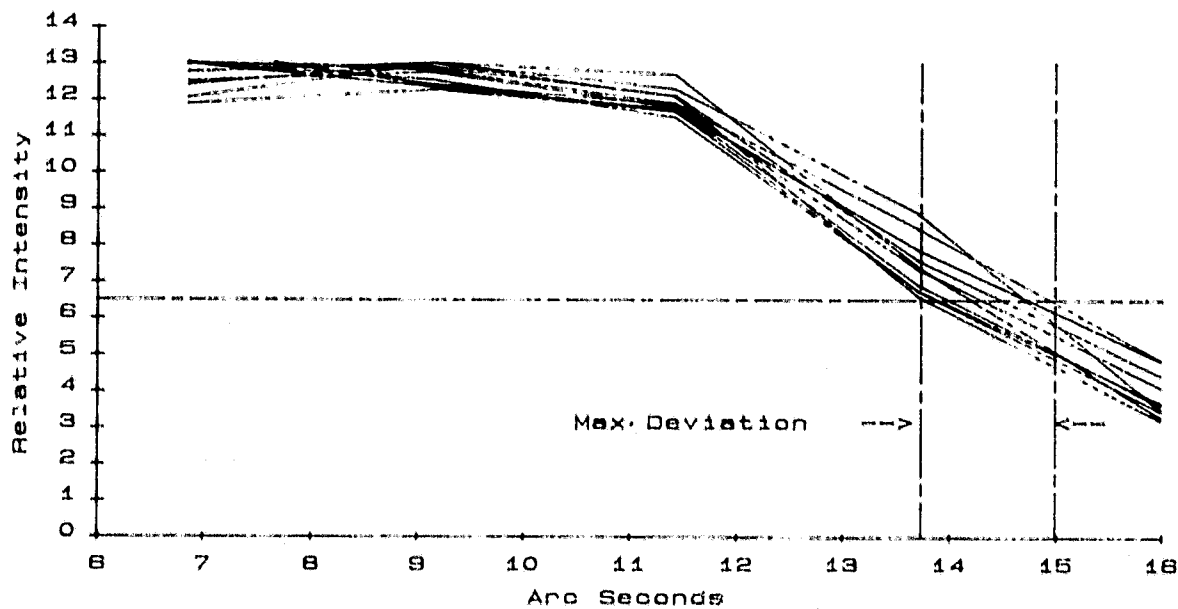


Figure 12. Enlargement of section A-A in Figure 11 showing image instability.

With further improvements such as closer electronic gain matching, camera alignments and tracking of the same spot groups as the co-located cameras is viewing, the stability obtainable with this approach could be improved. Analyses show that on a fully integrated system this concept should approach the basic stability of the tracker which is approximately 10-percent of the diffraction limit of the telescope. Assessment of this tracking system indicates that the tracking error is approximately 0.1

of the sunspot size. This is illustrated in Figures 11 and 12 where the spot size is shown to be approximately 1.3 arcsec and the maximum deviation is 1.4 arcsec. Tracking of smaller features such as solar granules is not possible because atmospheric seeing eliminates the image detail.

With space borne instruments the image detail will be greatly increased approaching the Rayleigh criterion for diffraction limit. Thus, fine detail such as the boundaries of granules would become available for image processing and would thereby allow tracker stability to approach 10 percent of the diffraction limit.

CONCLUSION

Extensive testing of solar area correlation and centroid tracking techniques has verified two concepts for stabilizing the image of a solar telescope by tracking directly in the focal plane. Both methods have comparable stability in the order of ± 0.6 arcsec while compensating telescope motion of up to 120 arcsec.

Although the correlation tracker system was primarily developed for solar telescopes, it has applications for space-based telescopes for aim point stabilization during Earth observations, and for aim point guidance of spacecraft during automated docking maneuvers.

This tracking system, as installed on the MSFC magnetograph, has enhanced the capability of the telescope by improving image quality and by increasing observation time during periods of wind induced perturbations.

REFERENCES

1. Breadboard Model Solar Correlation Tracker and Simulator: Final Summary Report, NAS8-29037, The Bendix Corporation/Mishawaka Operations for Marshall Space Flight Center, January 1973.
2. Design Data for Installation of Solar Area Correlation Tracker on a Solar Telescope, Technical Report AP-74840209, Bendix Aerospace Division, NAS8-31163, December 1974.
3. Evaluation of Motion Degraded Images: Seminar Report NAS SP-193, Cambridge, MA, December 1968, published 1969 by NASA/Office of Technology Utilization, Washington, D.C.
4. Proceedings of the IEEE: Digital Pattern Recognition, Vol. 60, Number 10, October 1972.
5. ATM Fine Sun Sensor System Description, MSFC 50M22156, NASA/MSFC, December 1970.
6. Solar Correlation Tracker Ground Testing, Annual and Semi-annual Reports, MSFC Director's Discretionary Fund, Project 49, Marshall Space Flight Center, 1980 through 1982.
7. Nesbitt Cumings, MSFC Correlation Tracker, Paper presented at the 156th Annual Meeting of the American Astronomical Society, University of Maryland, June 1980.
8. Field Support for Solar Correlation Tracker, Technical Report 5701-BLL-82-329, Bendix Guidance System Division, NAS8-346, July 1982.

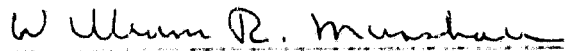
ORIGINAL PAGE IS
OF POOR QUALITY

APPROVAL

IMAGE MOTION COMPENSATION BY AREA CORRELATION AND
CENTROID TRACKING OF SOLAR SURFACE FEATURES

By M. F. Nein, W. R. McIntosh, and N. P. Cumings

The information in this report has been reviewed for technical content. Review of any information concerning Department of Defense or nuclear energy activities or programs has been made by the MSFC Security Classification Officer. This report, in its entirety, has been determined to be unclassified.


WILLIAM R. MARSHALL
Director, Program Development